IEEE Open Journal of
Intelligent Transportation
Systems

Received 26 March 2021; revised 28 May 2021 and 6 October 2021; accepted 17 December 2021. Date of publication 28 December 2021;
date of current version 11 January 2022.

Digital Object Identifier 10.1109/OJITS.2021.3138953

Universally Safe Swerve Maneuvers for Autonomous Driving

RYAN DE IACO, STEPHEN L. SMITH (Senior Member, IEEE), AND KRZYSZTOF CZARNECKI (Member, IEEE)

Department of Electrical and Computer Engineering, University of Waterloo, Waterloo, ON N2L 3G1, Canada

CORRESPONDING AUTHOR: R. DE IACO (e-mail: ryan.deiaco@uwaterloo.ca)

This work was supported by the Government of Ontario.

ABSTRACT This paper characterizes safe following distances for on-road driving when vehicles can avoid collisions by either braking or by swerving into an adjacent lane. In particular, we focus on safety as defined in the Responsibility-Sensitive Safety (RSS) framework. We extend RSS by introducing swerve maneuvers as a valid response in addition to the already present brake maneuver. These swerve maneuvers use the more realistic kinematic bicycle model rather than the double integrator model of RSS. When vehicles are able to swerve or brake, it is shown that their required safe following distance at higher speeds is less than that required through braking alone. In addition, when all vehicles follow this new distance, they are provably safe. The use of the kinematic bicycle model is then validated by comparing these swerve maneuvers to that of a dynamic single-track model. The analysis in this paper can be used to inform both offline safety validation as well as safe control and planning.

INDEX TERMS Autonomous vehicles, collision avoidance, intelligent vehicles, motion control, motion planning, vehicle safety.

I. INTRODUCTION

THE MAIN bottleneck for the public acceptance and ubiquity of autonomous driving is the current lack of safety guarantees. There are three main ways to establish the safety of an autonomous vehicle. The first involves measuring crash statistics over a large number of autonomously driven kilometers and comparing them to the equivalent human rates for each category of collision severity. However, particularly with severe collisions, the number of kilometers required to establish a statistically significant collision rate challenges the practical feasibility of this method for establishing safety.

An alternative method for determining the safety of a system is through scenario-based verification [1]. This method uses a set of scenarios that validate the vehicle's behavior across a representative set of situations. The goal is for the set of scenarios to capture most of the required driving behavior necessary for safe driving. However, it is difficult to construct such a set of scenarios that captures all of the challenging conditions faced by an autonomous vehicle [2].

A third approach for verifying the safety of a system is formally proving the behavior of a vehicle is safe [3]–[6]. In order to compute useful safety bounds, these works often include simplifying assumptions. The difficulty with this method lies in selecting reasonable assumptions to make. Generally, the stronger the assumptions made, the easier to prove the system is safe. However, if the assumptions are too strong, they may not hold in general driving scenarios. An additional challenge with this method is that to prove safety, the driving behavior may need to be conservative, or highly restrictive.

This paper aims to address the latter issue, especially as it pertains to the Responsibility-Sensitive Safety (RSS) framework [5]. The RSS framework prescribes safe longitudinal and lateral buffers between the autonomous vehicle and other vehicles on the road in order to guarantee safety under various assumptions. Fundamental to the RSS framework is its assumption of responsibility, and that vehicles have a duty

The review of this article was arranged by Associate Editor Pardis Khayyer.

This work is licensed under a Creative Commons Attribution 4.0 License. For more information, see https://creativecommons.org/licenses/by/4.0/

of care to one another. One of the fundamental claims of RSS is that if all agents follow this responsible duty of care towards one another, no collisions will occur. The assumption of responsible behavior allows for the autonomous vehicle to make meaningful progress in the driving task. Under other frameworks that assume adversarial vehicles, the autonomous vehicle often exhibits over-conservative behavior that impedes progress. This assumption of responsible behavior allows for the computation of safe following distances such that vehicles can comfortably brake for a braking vehicle in front of them, without causing a collision. This following distance is a function of both vehicles' speeds and maximum accelerations, as well as the reacting vehicle's reaction time. When computing this following distance, the vehicles are modeled by a kinematic particle model.

This paper extends this framework to include swerve maneuvers feasible for the kinematic bicycle model as a valid response, in addition to the standard braking response. In doing so, vehicles are able to follow at closer following distances at higher speeds, allowing for more efficient use of the road network. Using swerve maneuvers feasible for the kinematic bicycle model ensures that these maneuvers are more realistic than those possible under the particle model used in RSS. The simplicity of the bicycle model also allows for closed form solutions in our safe following distance bounds. While this paper does not prescribe a controller for this extended framework, it lays the groundwork for a given controller to reason about the decision between a swerving and braking response.

A. CONTRIBUTIONS

This article extends the work in our previous conference paper [7], which included the derivation of pairwise safe following distances between vehicles that swerve or brake when interacting with one another. This work is based on the RSS framework, and the evaluation of these distance bounds according to a dynamic single-track model. In this article, our first contribution is the review of the derivation of safe following distance bounds for vehicles swerving to avoid a braking vehicle and braking to avoid a swerving vehicle, with additional derivation details. We then introduce a new derivation for the safe following distance bound in the case of swerving to avoid a swerving vehicle. These safe distance bounds are then leveraged to derive a novel universal following distance that allows for smaller vehicle separation at high speeds as compared to the RSS framework. When all vehicles in a road network follow this new distance as well the rest of the RSS framework, and satisfy our assumptions, they are provably safe from collision.

The second contribution is a review of our validation of the use of the kinematic bicycle model by comparing our swerve maneuvers to maneuvers generated under a dynamic single-track model [8]. As part of this dynamic model, we include a Pacejka tire model [9] to account for road surface traction. We show that the kinematic model, when lateral acceleration is constrained, can accurately estimate the longitudinal distance required to perform swerve maneuvers using the dynamic model.

B. RELATED WORK

This work builds upon the RSS framework [5] which presents a closed form solution for the safe longitudinal and lateral distances between vehicles that brake according to a particle kinematic model when interacting with one another. An in-depth discussion on this work is presented in Section II-A.

Previous work on swerve maneuvers for autonomous driving have often focused on feasible maneuvers according to various kinodynamic models [10], [11]. In particular, many of these papers have assumed some variant of the bicycle model [12]–[15] and performed optimization to generate optimal swerve maneuvers. However, under these models the optimal solution is not generated through a closed form solution, which makes formally proving safety challenging. For the latter reason, assumptions and solutions in the RSS framework are stated in closed form.

Other work has instead simplified the vehicle model to a point mass model [16]–[18] in order to yield closed form, optimal solutions. However, this comes at the cost of the nonholonomic constraint present in the bicycle model, which results in maneuvers that would be unrealistic for a car to execute. The goal with this work is to yield closed form, feasible solutions to swerve maneuver boundary condition problems, while still preserving the kinematic constraints that allow the maneuver to be executable by a real vehicle.

To prove maneuver safety under specified control limits, one approach has been to use reachability analysis [3], [6], [19], [20], in which the full reachable space of agents is considered when generating evasive maneuvers. These methods have been integrated into motion planners with success [21], although the pessimistic assumptions made about adversarial agent behavior can limit the effectiveness of the planning algorithms in dense driving conditions.

Previous work on using the kinematic bicycle model for autonomous driving has shown that it is an effective model for tracking trajectories in MPC [22], and as such, contains important kinematic constraints that capture some of the limits of vehicle motion. Past work has also shown that the kinematic bicycle model is an accurate approximation to vehicle motion at low accelerations [23], which we expect to see as well in our validation. Note that braking and swerving in RSS are not emergency maneuvers, which would necessitate high accelerations. RSS instead focuses on maintaining following distances that allow comfortable acceleration levels during avoidance maneuvers.

II. PRELIMINARIES

A. RESPONSIBILITY-SENSITIVE SAFETY (RSS)

In this paper, we rely on two aspects of the RSS framework; the longitudinal and lateral safe distances required between two vehicles. In particular, we examine how the equivalent longitudinal safe distance for a swerve maneuver compares

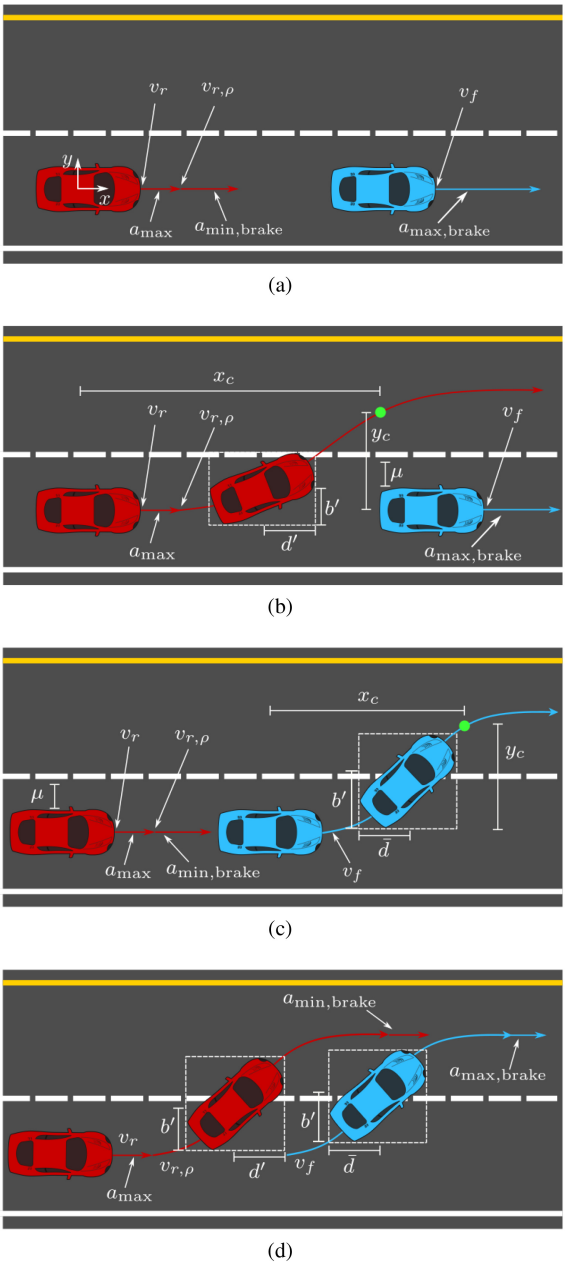

FIGURE 1. **(a) The standard RSS braking maneuver for a braking front vehicle. Velocity and acceleration arrows point to path segments where they occur. (b) The proposed swerve maneuver for a braking front vehicle. The green dot represents the lateral clearance distance y_c required by RSS. (c) The braking maneuver required for a swerving front vehicle. (d) The swerving maneuver required for a swerving front vehicle.**

to that of a brake maneuver, while maintaining an appropriate lateral safe distance when required. In this work, we compare swerve maneuvers moving to the left of the front vehicle, as in Figure 1 (safe distances are computed for the red car); however, the same analysis can be applied to swerves moving to the right.

In RSS, safe distances are a function of several variables that describe the situation. The initial speed of the rear autonomous vehicle is given by v_r, and the initial speed of the front vehicle is denoted by v_f. The reaction time is given by ρ. The interpretation of the reaction time is the duration after which a vehicle can apply a mitigating action. During the reaction time, both vehicles apply the most dangerous acceleration possible, $a_{\max,\text{accel}}$, $a_{\max,\text{brake}}$ in the longitudinal case, and $a^{\text{lat}}_{\max}$ in the lateral case. To ensure passenger comfort, as well as to prevent tailgater safety issues, the mitigating reaction of the rear vehicle is assumed to be a comfortable deceleration, denoted $a_{\min,\text{brake}}$. This term comes from RSS, and is interpreted as the threshold for a safe, responsible braking response for the autonomous car. Note that these accelerations are magnitudes.

We denote the positive part of an expression with $[\,\cdot\,]_+$. Velocities are signed according to Figure 1(a), and accelerations are unsigned parameters of the framework. If the post-reaction speeds $v_{r,\rho}$ and $v_{f,\rho}$ are given by

$$v_{r,\rho} = v_r + a_{\max,\text{accel}}\rho, \tag{1}$$
$$v^{\text{lat}}_{r,\rho} = v^{\text{lat}}_r - a^{\text{lat}}_{\max}\rho, \tag{2}$$
$$v^{\text{lat}}_{f,\rho} = v^{\text{lat}}_f + a^{\text{lat}}_{\max}\rho, \tag{3}$$

the *longitudinal and lateral safe distances* are given by

$$d_{\text{long}} = \left[v_r\rho + \frac{1}{2}a_{\max,\text{accel}}\rho^2 + \frac{v^2_{r,\rho}}{2a_{\min,\text{brake}}} - \frac{v^2_f}{2a_{\max,\text{brake}}} \right]_+, \tag{4}$$

$$d_{\text{lat}} = \mu + \left[-\frac{v^{\text{lat}}_r + v^{\text{lat}}_{r,\rho}}{2}\rho + \frac{\left(v^{\text{lat}}_{r,\rho}\right)^2}{2a^{\text{lat}}_{\min}} + \frac{v^{\text{lat}}_f + v^{\text{lat}}_{f,\rho}}{2}\rho + \frac{\left(v^{\text{lat}}_{f,\rho}\right)^2}{2a^{\text{lat}}_{\min}} \right]_+. \tag{5}$$

The longitudinal safe distance is between the frontmost point of the rear vehicle and the rearmost point of the front vehicle along the longitudinal direction, and the lateral safe distance is between the rightmost point of the rear vehicle and the leftmost point of the front vehicle along the lateral direction. These are left implicit in the original RSS formulation, but since swerves involve rotation of the chassis, we make them explicit in this work. The longitudinal safe distance d_{long} is the distance required such that the rear vehicle can maximally accelerate during its reaction time, then minimally decelerate to a stop, all while the front vehicle is maximally braking, without causing a collision. The lateral safe distance d_{lat} is the distance required such that both vehicles can maximally accelerate towards each other during the reaction time ρ, then minimally decelerate until zero lateral velocity, while still maintaining at least a μ distance buffer.

When computing safety for swerve maneuvers, the vehicle must maintain these safe distances with other relevant vehicles. These vehicles are relevant according to longitudinal and lateral adjacency, as defined below. We denote the vehicle dimensions d_f, d_r, b_l, b_r as in Figure 3(a). The black dot in Figure 3(a) will be a standard reference point

for our bicycle model, which can also represent the center of mass. However, it could be moved elsewhere along the wheelbase axis if needed. We assume all vehicles have the same dimensions for simplicity, but this can be easily generalized.

Definition 1: If x_1, x_2 denote the longitudinal position of each vehicle, and then the vehicles are *laterally adjacent* if $x_2 - d_r - d_f \leq x_1 \leq x_2 + d_r + d_f$.

Definition 2: If y_1, y_2 denotes the lateral position of each vehicle, then the vehicles are *longitudinally adjacent* if $y_2 - b_l - b_r - d_{lat} \leq y_1 \leq y_2 + b_l + b_r + d_{lat}$.

Combining the definitions for safe distances and adjacency gives us a definition of safety.

Definition 3: A vehicle is *laterally/longitudinally safe* from another vehicle if it is not laterally/longitudinally adjacent to the other vehicle, or if it is laterally/longitudinally adjacent to the other vehicle and there is at least $d_{\text{lat}}/d_{\text{long}}$ of distance between them.

Definition 4: For a swerving vehicle and a non-swerving vehicle, as well as a given swerve maneuver, we define the *lateral clearance distance*, y_c, as the earliest point in the swerve at which the swerving vehicle is no longer longitudinally adjacent to the non-swerving vehicle.

In Figure 1, y_c is reached at the green dot along the swerve. Note that before this point y_c, the vehicles are not laterally adjacent. The lateral clearance distance allows us to compute the longitudinal distance covered by the swerve, which is denoted by x_c. We then use x_c to compute the equivalent of d_{long} for a swerve maneuver, and compare it to Equation (4). Since we are using a swerve maneuver, the definition of longitudinal adjacency will incorporate additional buffer distance to compensate for the change in chassis yaw during swerving. This is discussed in detail in Section IV-A.

B. VEHICLE MODELS

The analysis in this paper relies upon three different kinodynamic models. The first is the particle kinematic model, which is used in the RSS framework. Through all of these kinodynamic models, x is longitudinal displacement and y is lateral displacement. The control input for the particle kinematic model is the acceleration in each dimension

$$\ddot{x} = a_x, \quad \ddot{y} = a_y. \tag{6}$$

When computing swerve maneuvers, we wish to model the non-holonomic constraints on a car's motion to make the maneuvers realistic. To do so, we rely on the kinematic bicycle model, a model commonly used in autonomous driving [22], [24], [25]. This is illustrated in Figure 2(a). In this model, v is the velocity of the vehicle, ψ is the heading of velocity at the center of mass, θ is the yaw of the chassis, β is the slip angle of the center of mass relative to the chassis, δ is the input steering angle, R_c is the turning radius of the center of mass, and l_r and l_f are the distances from the rear

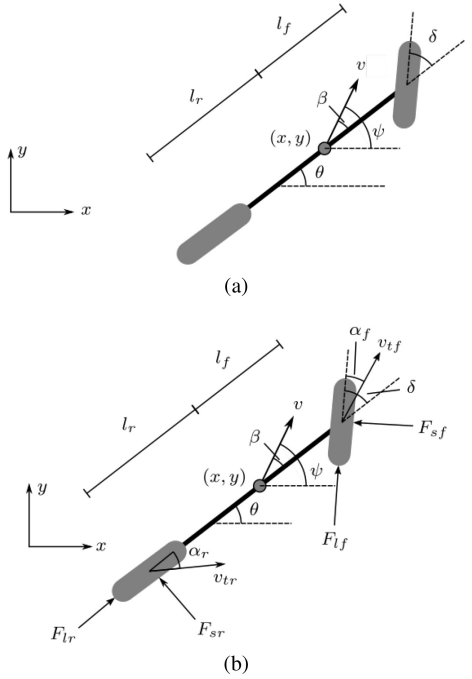

FIGURE 2. (a) The kinematic bicycle model, along with its associated variables. (b) The dynamic single track model used for validation [8]. Drag forces are omitted for simplicity, but are included in our computation.

and front axle to the center of mass, respectively:

$$\begin{aligned}
\dot{x} &= v\cos(\psi + \beta), \quad \beta = \tan^{-1}\left(\frac{l_r}{l_r + l_f}\tan(\delta)\right),\\
\dot{y} &= v\sin(\psi + \beta), \quad \theta = \psi - \beta,\\
\dot{\theta} &= \frac{v\tan(\delta)}{l_r + l_f}, \quad |\delta| \leq \delta_{\max},\\
|a_{\text{lat}}| &= \frac{v^2}{R_c} \leq a^{\text{lat}}_{\min}, \quad -a_{\min,\text{brake}} \leq a \leq a_{\max}\\
R_c &= \frac{l_r + l_f}{\cos(\beta)\tan(\delta)}.
\end{aligned} \tag{7}$$

Note that we use $a^{\text{lat}}_{\min}$ when constraining the vehicle's lateral acceleration, as we want to analyze guaranteed performance during the swerve maneuver, whereas we use $a^{\text{lat}}_{\max}$ in Equation (5) to be conservative about the possible action from both vehicles during the reaction delay ρ. One should select $a^{\text{lat}}_{\min}$ to ensure comfort and stability during the swerve maneuver.

Finally, to verify our kinematic approximation is valid, we compare our swerve maneuvers to those executed by a dynamic single-track vehicle model [8] with tires modeled using the Pacejka tire model [9]. This model is shown in Figure 2(b). In this vehicle model, v, ψ, β, δ, l_f, and l_r are the same as the bicycle model. The slip angles of the front and rear tires are α_f and α_r, respectively. The lateral tire forces on the front and rear tires are denoted F_{sf} and F_{sr}, respectively, and F_{lf} and F_{lr} denote the longitudinal tire forces at the front and rear tires, respectively. The drag mount point is denoted e_{SP}, and F_{Ax} and F_{Ay} are the longitudinal and lateral

drag forces, respectively. The yaw rate is ω_z, and ω_δ is the input steering rate. The mass of the car is m, and I_{zz} is the inertia about the z-axis. We omit the equations of motion for brevity, but they are presented in the Reference [8].

III. PROBLEM FORMULATION

The fundamental problem this paper addresses is to compute the longitudinal safe distance required when there is a free lane (or shoulder) to the left or right of the vehicle, allowing for an evasive swerve maneuver. This requires knowing the longitudinal safe distance required for the scenarios illustrated in Figure 1. As can be seen, when computing the longitudinal safe distances for swerves, one needs to consider both longitudinal and lateral clearance, since swerves involve lateral and longitudinal displacement.

Since vehicles rotate during swerves, rotation must be compensated for when computing these clearances. After compensating for rotation, the longitudinal swerve distance x_c can then be used to compute the longitudinal safe distance required for a swerve. In RSS, safety was proved for a particle model. This paper extends those results to prove the safety for swerves feasible for the kinematic bicycle model. It is then shown how this result can be applied to more general models in Section V. This task then breaks down into five subproblems.

Subproblem 1: Given the initial speed of a swerving vehicle v_r, the vehicle dimensions d_f, d_r, b_l, b_r as in Figure 3(a), and parameters μ and ρ, compute a lateral clearance distance y_c sufficient for lateral safety when a swerving vehicle becomes laterally adjacent to a lead vehicle.

Subproblem 2: Given the kinematic constraints in (7), the initial vehicle speeds v_r and v_f, the lateral clearance distance y_c, and parameters ρ, $a_{\max}$, $a_{\min,\text{brake}}$, $a_{\max,\text{brake}}$, $a^{\text{lat}}_{\max}$, and $a^{\text{lat}}_{\min}$, compute a longitudinal safe distance sufficient for safety when swerving for a braking lead vehicle. This is illustrated in Figure 1(b).

Subproblem 3: Given the initial vehicle speeds v_r and v_f, the clearance point y_c, and parameters ρ, $a_{\max}$, $a_{\min,\text{brake}}$, $a^{\text{lat}}_{\max}$, and $a^{\text{lat}}_{\min}$, compute a longitudinal safe distance sufficient for safety when braking for a swerving lead vehicle. This is illustrated in Figure 1(c).

Subproblem 4: Given the kinematic constraints in (7), the initial vehicle speeds v_r and v_f, the parameters ρ, $a_{\max}$, $a_{\min,\text{brake}}$, $a_{\max,\text{brake}}$, $a^{\text{lat}}_{\max}$, and $a^{\text{lat}}_{\min}$, compute a longitudinal safe distance sufficient for safety when swerving behind a swerving lead vehicle. This is illustrated in Figure 1(d).

Subproblem 5: Given longitudinal safe distance sufficient for safety when swerving for a braking vehicle, braking for a swerving lead vehicle, and swerving for a swerving lead vehicle, compute a longitudinal safe distance akin to d_{long} that is sufficient for universal safety when maintained by all vehicles on the road.

The first subproblem is addressed in Section IV-A, the second in Section IV-B, the third in Section IV-C, the fourth in Section IV-D, and the fifth in Section IV-E.

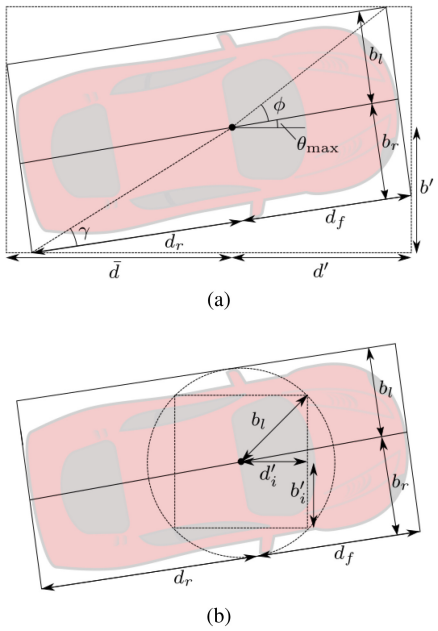

FIGURE 3. (a) An outer approximation to a vehicle chassis that rotates by $\theta_{\max}$. The distances d' and $\bar{d}$ are used for longitudinal buffers during swerve maneuvers, and b' is used as a lateral buffer. (b) An inner approximation to a rotating vehicle chassis.

The work in this paper makes the following assumptions on responsible behavior:

1) A vehicle will only perform a swerve maneuver if it is not braking, and will only perform a brake maneuver if it is not swerving.
2) For every swerve maneuver, each vehicle reaches the lateral clearance distance only once. As a result, once a vehicle has committed to a lane change by reaching the lateral clearance distance, it will not return to its previous lane.
3) Each vehicle moves forward along the road, $v \geq 0$ and $\frac{-\pi}{2} \leq \psi \leq \frac{\pi}{2}$.

IV. COMPUTING THE LONGITUDINAL SAFE DISTANCE

In this section, we compute longitudinal safe distance to a lead vehicle required during a swerve maneuver. To do so, we first compute the lateral clearance from the lead vehicle required for safety, and then use this to compute the longitudinal safe distance according to the geometry of the swerve maneuver.

A. LATERAL CLEARANCE DISTANCE

To compute the lateral clearance distance y_c, we modify Equation (5) to account for vehicle rotation. If we know the maximum chassis yaw $\theta_{\max}$ during the maneuver, we can compute an axis-aligned bounding rectangle as an outer approximation to the vehicle footprint. This is useful for safety analysis, as we can now bound the swept area during the maneuver, which is illustrated in Figure 3(a).

The three distances we need for safety analysis are from the center of mass to the front of the bounding rectangle, d';

from the center of mass to the side of the bounding rectangle, b'; and from the center of mass to the rear of the bounding rectangle, $\bar{d}$. The distances from the center of mass to the rear and front of the chassis are d_r and d_f, respectively. The distances to the left and right of the chassis are b_l and b_r, respectively.

As the vehicle rotates, each corner of the oriented bounding rectangle pushes outwards the side of the axis-aligned bounding rectangle that it touches until the line connecting the corner with the center becomes perpendicular to the side. Further rotation past each of these angles decreases the corresponding dimensions of the axis-aligned bounding rectangle. We can write these angles in terms of $\theta_{\max}$, ϕ, and γ, illustrated in Figure 3(a). The equations for the bounding rectangle distances are then d', $\bar{d}$, and b' are

$$d' = \begin{cases} d_f \cos(\theta_{\max}) + b_r \sin(\theta_{\max}) & \theta_{\max} \leq \phi, \\ \sqrt{d_f^2 + b_r^2} & \theta_{\max} > \phi, \end{cases} \tag{8}$$

$$\bar{d} = \begin{cases} d_r \cos(\theta_{\max}) + b_l \sin(\theta_{\max}) & \theta_{\max} \leq \gamma, \\ \sqrt{d_r^2 + b_l^2} & \theta_{\max} > \gamma, \end{cases} \tag{9}$$

$$b' = \begin{cases} d_r \sin(\theta_{\max}) + b_r \cos(\theta_{\max}) & \theta_{\max} \leq \frac{\pi}{2} - \gamma, \\ \sqrt{d_r^2 + b_r^2} & \theta_{\max} > \frac{\pi}{2} - \gamma. \end{cases} \tag{10}$$

We now have an expression for the bounding rectangle distances of a rotating vehicle in terms of $\theta_{\max}$, which is computed in Section IV-B.

Using b' and the lateral safe distance d_{lat}, we can now compute the lateral clearance distance, y_c required for Subproblem 1.

$$y_c = b' + b_l + d_{\text{lat}}. \tag{11}$$

Let us denote the time y_c is attained as t_c.

Theorem 1: Equation (11) gives a lateral clearance distance sufficient for lateral safety when a swerving vehicle becomes laterally adjacent to another braking vehicle, or any time before.

Proof: To show lateral safety, we must show that laterally adjacent vehicles are at least d_{lat} from one another, as given in Equation (5). Since the swerving vehicle's lateral speed is variable but nonnegative, a conservative lower bound on its lateral velocity is zero when computing d_{lat}. From assumption 1, since the other vehicle is braking, it is not swerving, and therefore has zero lateral velocity during the swerve. The required d_{lat} can then be computed using Equation (5), taking v_r^{lat} and v_f^{lat} to be zero, and using the parameters $a_{\min}^{\text{lat}}$, $a_{\max}^{\text{lat}}$, and ρ. The distance d_{lat} acts as a buffer to ensure that upon reaching lateral adjacency, both agents are laterally safe from one another.

For $t < t_c$, the swerving vehicle is not laterally adjacent to the other vehicle, and is laterally safe. For $t \geq t_c$, from Assumption 2, t_c is the time at which the two vehicles are closest while laterally adjacent. From Equation (11), there is at least d_{lat} of distance between the vehicles, and thus they are laterally safe $\forall t \geq t_c$. ■

B. SWERVING FOR A BRAKING VEHICLE

We can now use y_c to compute the longitudinal safe distance, $d_{s,b}$, required when swerving to avoid a braking lead vehicle. We wish to do so under the constraints of the bicycle model outlined in Section II-A. In addition, if α denotes the lane width, t_f denotes the end time of the swerve, and the origin of the coordinate frame is at the center line of the current lane at the rear vehicle's position at $t = 0$, we would like the swerve to satisfy the following boundary conditions:

$$\theta(t_f) = 0, \;\; y(t_f) = \alpha. \tag{12}$$

However, to compute the optimal swerve maneuver with respect to longitudinal clearance is an optimization problem with no closed form solution [13]. Instead, we can compute a swerve maneuver feasible for the bicycle model, and use that to obtain an upper bound on the actual longitudinal distance required by a swerve constrained by the bicycle model.

As in Equation (4), the lead vehicle is traveling with velocity v_f, and then brakes at $a_{\max,\text{brake}}$ during the entire maneuver. The swerve is preceded by the rear vehicle maximally accelerating during the reaction delay ρ, at which point it begins the swerve maneuver with initial speed $v_{r,\rho}$. To ensure monotonicity in the gap between the rear and lead vehicles, a lower bound on the distance traveled until t_f by the lead vehicle is used, denoted x_f. We will rely on this monotonic property when proving Theorem IV-B.2.

The swerve we consider is bang-bang in the steering input with zero longitudinal acceleration, and is illustrated in Figure 4. Note that the bang-bang steering input leads to an unsmooth transition in steering angle between the two arcs of the swerve. This is permissible under our selected bicycle model, and is reasonable for small steering angles. Allowing bang-bang steering angles without a smooth transition between the arcs of our swerve formulation will allow for closed form solutions to the problems discussed in the rest of Section IV. We denote the longitudinal distance traveled by the swerving vehicle until the swerving vehicle reaches the lateral clearance distance as x_c This distance x_c is computed in Equations (21) and (26).

For the swerve maneuver, the turning radius of the circular arcs depends on the maximum lateral acceleration, as well as the kinematic limits of the steering angle. The constraints on steering angle and lateral acceleration from (7) give two constraints on the turning radius

$$R_{\min,\delta} = \sqrt{\frac{(l_r + l_f)^2}{\tan(\delta_{\max})^2} + l_r^2}, \quad R_{\min,a} = \frac{v_{r,\rho}^2}{a_{\min}^{\text{lat}}}. \tag{13}$$

To ensure both constraints are satisfied, we set R_c from (7) to the maximum of the two. From this turning radius, we can compute the steering angle δ_c and the slip angle β_c

$$\delta_c = \tan^{-1}\left(\sqrt{\frac{(l_r + l_f)^2}{R_c^2 - l_r^2}}\right), \quad \beta_c = \tan^{-1}\left(\frac{l_r \tan(\delta_c)}{l_r + l_f}\right). \tag{14}$$

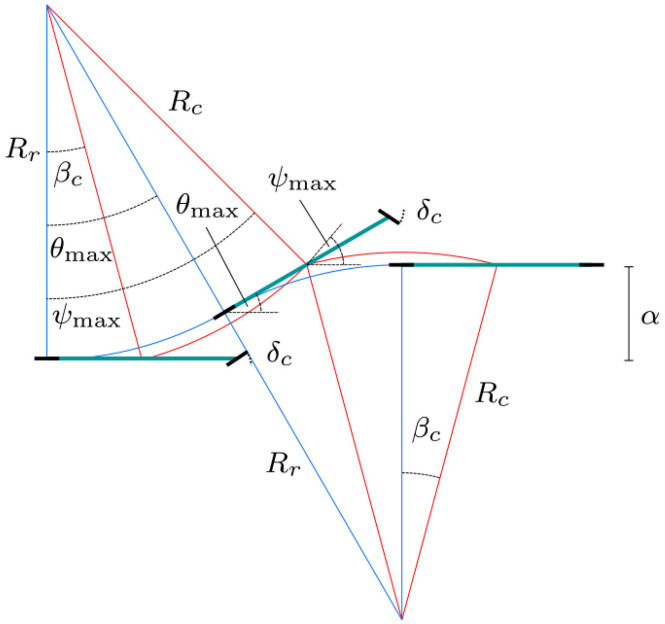

FIGURE 4. The swerve maneuver used for safety analysis. The red path is taken by the center of mass, and the blue path is taken by the rear axle. The distance between lanes is α, δ_c is the steering angle, β_c is the slip angle. The maximum angles achieved by the chassis yaw and the velocity of the center of mass are given by $\theta_{\max}$ and $\psi_{\max}$, respectively. The turning radius of the rear axle and center of mass's paths are given by R_r and R_c, respectively.

We can now compute the $\theta_{\max}$ required to satisfy the boundary conditions in Equation (12). From the rear axle, the two circular arcs are symmetrical in lateral distance traveled, as in Figure 4. Therefore, we can compute the angle along the first circular arc required to reach a lateral distance of $\frac{\alpha}{2}$. First, we compute the turning radius at the rear axle, R_r

$$R_r = \frac{l_r + l_f}{\tan(\delta_c)}. \tag{15}$$

The lateral distance traveled during the first circular arc is then given by

$$y(t) = R_r(1 - \cos(\theta(t))). \tag{16}$$

For a given value of δ_c, $\theta_{\max}$ is then

$$\theta_{\max} = \cos^{-1}\left(1 - \frac{\alpha}{2R_r}\right). \tag{17}$$

To compute x_c, there are two cases, depending on if y_c is reached in the first or second circular arc. We can compute $\psi_{\max}$ using (7). From Assumption 3, we have that $\psi_{\max} \leq \frac{\pi}{2}$. Thus, the first case occurs if

$$y_c \leq R_c(\cos(\beta_c) - \cos(\psi_{\max})), \tag{18}$$

otherwise the second case occurs.

1) FIRST CIRCULAR ARC

Similar to Equation (16), the longitudinal position along the first circular arc is given by

$$x(t) = R_c(\sin(\psi(t)) - \sin(\beta_c)). \tag{19}$$

We can use the center of mass equivalent of Equation (16) and y_c to compute the ψ value at the clearance point, ψ_c

$$\psi_c = \cos^{-1}\left(\cos(\beta_c) - \frac{y_c}{R_c}\right). \tag{20}$$

Substituting this value for ψ in Equation (19) gives our swerve longitudinal distance

$$x_c = R_c(\sin(\psi_c) - \sin(\beta_c)). \tag{21}$$

The magnitude of the velocity is constant during the swerve, and so we can compute t_c using the arc length traveled up to the clearance point y_c,

$$t_c = \frac{R_c(\psi_c - \beta_c)}{v}. \tag{22}$$

2) SECOND CIRCULAR ARC

In the second circular arc, taking $\psi_{\max} = \theta_{\max} + \beta_c$, we denote the initial heading of the center of mass as $\hat{\psi} = \psi_{\max} - 2\beta_c$, the initial x position as $\hat{x} = R_c(\sin(\psi_{\max}) - \sin(\beta_c))$, and the initial y position as $\hat{y} = R_c(\cos(\beta_c) - \cos(\psi_{\max})$. The longitudinal and lateral distance along this arc are then

$$x(t) = R_c\left(\sin\left(\hat{\psi}\right) - \sin(\psi(t))\right) + \hat{x}, \tag{23}$$

$$y(t) = R_c\left(\cos(\psi(t)) - \cos\left(\hat{\psi}\right)\right) + \hat{y}. \tag{24}$$

As in Case 1, substituting y_c in Equation (24) gives us ψ_c,

$$\psi_c = \cos^{-1}\left(\frac{1}{R_c}(y_c - \hat{y}) + \cos(\hat{\psi})\right) \tag{25}$$

Substituting this value for ψ in Equation (23) and adding d' gives

$$x_c = R_c\left(\sin\left(\hat{\psi}\right) - \sin(\psi_c)\right) + \hat{x}. \tag{26}$$

Similar to Case 1, we can then compute the clearance time t_c,

$$t_c = \frac{R_c\left(\psi_{\max} - \beta_c + \hat{\psi} - \psi_c\right)}{v}. \tag{27}$$

From these longitudinal swerve clearance values, we can then compute the longitudinal safe distance. To do this, we can replace the rear braking distance in Equation (4) with the longitudinal swerve distance x_c. In addition, to ensure a monotonically decreasing gap between the two vehicles, we set the initial speed of the lead vehicle (as a conservative approximation) to

$$v_f' = \min\left(v_f, v_r\cos(\psi_{\max})\right). \tag{28}$$

The braking distance of the lead vehicle occurs during the reaction time ρ and the swerve clearance time t_c, giving a front vehicle braking distance of

$$x_f = v_f'(\rho + t_c) - \frac{a_{\max,\text{brake}}(\rho + t_c)^2}{2}. \tag{29}$$

Using the parameters $a_{\max,\text{accel}}, \rho$ introduced in Section II-A, the longitudinal safe distance between a swerving rear vehicle and a braking lead vehicle is

$$d_{s,b} = \left[v_r \rho + \frac{1}{2} a_{\max,\text{accel}} \rho^2 + x_c - x_f \right]_+ + d' + d. \quad (30)$$

Theorem 2: Equation (30) gives a longitudinal safe distance sufficient for safety when swerving for a braking lead vehicle.

Proof: For $t > t_c$, $y(t) > y_c$, and therefore the swerving vehicle is no longer longitudinally adjacent to the lead vehicle, so is safe from the lead vehicle's braking. For $t \leq t_c$, from Equation (28), we use a conservative lower bound for the speed of the lead vehicle to ensure the lead vehicle's speed is less than the swerving vehicle's speed during the entire swerve. This implies the gap between the two vehicles is monotonically decreasing. This means the minimum gap between the two vehicles occurs at time t_c.

The swerving vehicle travels $x_c + v_r \rho + \frac{1}{2} a_{\max,\text{accel}} \rho^2$, and a conservative lower bound on the lead vehicle's travel distance is $v'_f(\rho + t_c) - \frac{1}{2} a_{\max,\text{brake}} (\rho + t_c)^2$. There is at most d' of distance from the center of mass to the front of the swerving vehicle. Thus, if a swerving vehicle maintains distance $d_{s,b}$, it is safe from the lead vehicle at time t_c. Since the gap is monotonically decreasing for $t \leq t_c$, it is safe $\forall t \leq t_c$. ■

C. BRAKING FOR A SWERVING VEHICLE

The longitudinal safe distance required to swerve for a braking vehicle was computed in the preceding section, and this section considers the opposite problem, computing the longitudinal safe distance required to brake for a swerving lead vehicle without collision. It is assumed the front vehicle is performing the same swerve discussed in Section IV-B. To account for rotation of the front vehicle, $\bar{d}$ is used to compensate as defined in Section IV-A.

Equations (21), (22), (26), and (27) can be used to compute the x_c and t_c for the front vehicle's swerve. As in Equation (4), it is assumed that the rear vehicle accelerates maximally during its reaction time, and then brakes comfortably until t_c. As before, denote the rear vehicle's post-acceleration velocity as $v_{r,\rho}$. Then its minimum velocity during the braking maneuver is

$$v_{r,\min} = \left[\min\left(v_r, v_{r,\rho} - a_{\min,\text{brake}} (t_c - \rho) \right) \right]_+. \quad (31)$$

As in Section IV-B, the proof of safety is simplified if the gap is monotonically decreasing until lateral safety is reached. To ensure this, the lead vehicle speed is conservatively bounded with v'_f

$$v'_f = \min\left(v_f \cos(\psi_{\max}), v_{r,\min} \right). \quad (32)$$

A conservative lower bound for the longitudinal distance traveled by the swerving front vehicle is then

$$x_f = v'_f t_c. \quad (33)$$

The distance x_f is a lower bound on the distance traveled by the front vehicle during the swerve that creates a monotonically decreasing gap.

The distance traveled by the rear braking vehicle during its reaction delay and its braking maneuver is denoted by x_r. This distance depends on the clearance time t_c, similar to the distance traveled by the front vehicle in the preceding section. The distance traveled during the rear vehicle's braking maneuver, $x_{r,\text{brake}}$, is given by

$$x_{r,\text{brake}} = \begin{cases} v_{r,\rho}(t_c - \rho) - \frac{a_{\min,\text{brake}} (t_c - \rho)^2}{2}, & t_c - \rho \leq \frac{v_{r,\rho}}{a_{\min,\text{brake}}}, \\ \frac{v_{r,\rho}^2}{2 a_{\min,\text{brake}}}, & t_c - \rho > \frac{v_{r,\rho}}{a_{\min,\text{brake}}}. \end{cases} \quad (34)$$

The first case occurs when the front agent reaches lateral safety from the rear agent before the rear agent can come to a complete stop. Otherwise the second case occurs.

Following this, the distance traveled by the braking rear vehicle is

$$x_r = \frac{(v_r + v_{r,\rho})\rho}{2} + x_{r,\text{brake}}. \quad (35)$$

Using Equations (33) and (35), the longitudinal safe distance when braking for a swerving vehicle, $d_{b,s}$ is then

$$d_{b,s} = \left[x_r - x_f \right]_+ + d_f + \bar{d}. \quad (36)$$

Theorem 3: Equation (36) gives a longitudinal safe distance sufficient for safety when braking for a swerving lead vehicle.

Proof: For $t > t_c$, the swerving vehicle is laterally clear from the rear braking vehicle, and therefore the rear vehicle is safe. The velocity used for the lead vehicle is a conservative lower bound on its true speed $\forall t \leq t_c$, as per Equation (32). In addition, $v'_f \leq v_r$, $\forall t \leq t_c$, and as a result the gap between the two vehicles is monotonically decreasing on that interval. The minimum distance between the two vehicles thus occurs at time t_c. Equation (36) thus gives enough clearance such that no collision occurs at time t_c, so the rear vehicle is safe at time t_c. Since the gap is monotonically decreasing over the interval, the rear vehicle is safe $\forall t \leq t_c$. ■

D. SWERVING FOR A SWERVING VEHICLE

The final relevant longitudinal safe distance is the distance required when swerving behind a swerving lead vehicle. This is illustrated in Figure 1(d). Both vehicles are longitudinally adjacent during the entire maneuver. From Assumption 1, the lead vehicle will not brake during its swerve. The goal is then to compute the longitudinal distance required to swerve behind a lead swerving vehicle, such that if the lead vehicle were to immediately brake with deceleration $a_{\max,\text{accel}}$ at the end of its swerve, and the rear vehicle were to brake with deceleration $a_{\min,\text{accel}}$ at the end of its reaction-delayed swerve, there would be no collision. The swerve completion times of the rear and front vehicle are given by t_1 and t_2, respectively. Similar to the previous section, v'_f denotes a conservative lower bound on the front vehicle's speed. The longitudinal safe distance required to swerve in response to

a swerving vehicle, $d_{s,s}$, is then

$$t_1 = \frac{2R_c\theta_{\max}}{v_r,\, \rho}, \quad t_2 = \frac{2R_c\theta_{\max}}{v_f} \tag{37}$$

$$d_{s,s} = \frac{v_r + v_{r,\rho}}{2}\rho + v_{r,\rho}t_1 + \frac{v_{r,\rho}^2}{2a_{\min,\text{brake}}} - \left(v_f' t_2 + \frac{v_f'^2}{2a_{\max,\text{brake}}}\right) + d' + \bar{d}. \tag{38}$$

Theorem 4: Equation (38) gives a longitudinal safe distance sufficient for safety when swerving for a swerving lead vehicle.

Proof: The gap between each vehicle can be written as a piecewise function of time. The endpoints of the intervals are functions of the reaction delay, ρ; the duration of the front vehicle's swerve, t_2; the duration of the rear vehicle's swerve, t_1; the brake duration of the front vehicle, $t_{b,2}$; and the brake duration of the rear vehicle, $t_{b,1}$. The swerve times for the kinematic bicycle model for varying speeds are proportional to $v\cos^{-1}(1-\frac{1}{v^2})$, which is quasi-constant across all relevant road speeds. In addition, $a_{\max,\text{accel}} > a_{\min,\text{accel}}$, and swerve times are longer than reasonable reaction times. From this, it is reasonable to assume that the interval endpoints are $\rho < t_2 < \rho + t_1 < t_2 + t_{b,2} < \rho + t_1 + t_{b,1}$. Denote the longitudinal distance traveled during the swerves by the front and rear vehicle as $x_{s,2}(t)$ and $x_{s,1}(t)$ respectively, the initial gap between the vehicles by g_0, and the gap between the vehicles as $g(t)$.

The maximum longitudinal velocity during the rear vehicle swerve is $v_{r,\rho}$. If the maximum ψ value during the front vehicles swerve is denoted $\psi_{\max,f}$, the minimum longitudinal velocity during the front vehicle's swerve is given by $v_f\cos(\psi_{\max,f})$. Set $v_f' = \min(v_f\cos(\psi_{\max,f}), v_r)$. This means that

$$x_{s,1}(t) \le v_{r,\rho}t, \tag{39}$$

$$x_{s,2}(t) \ge v_f' t. \tag{40}$$

Using Equations (39) and (40) as conservative bounds on the distance traveled by both vehicles during the swerve maneuver results in a monotonically decreasing function of t, $\hat{g}(t)$, with the property that $\hat{g}(t) \le g(t), \forall t$.

This implies that the minimum of $\hat{g}(t)$ occurs for $t > \rho + t_1 + t_{b,1}$, where $\hat{g}(t)$ is constant

$$\min_t \hat{g}(t) = g_0 + v_f' t_2 + \frac{v_f'^2}{2a_{\max,\text{brake}}} - \left(\frac{v_r + v_{r,\rho}}{2}\rho + v_{r,\rho}t_1 + \frac{v_{r,\rho}^2}{2a_{\min,\text{brake}}}\right). \tag{41}$$

Since $\hat{g}(t) \le g(t), \forall t$, if $\hat{g}(t) \ge 0, \forall t$, no collision occurs. This is satisfied if the initial gap satisfies

$$g_0 \ge \frac{v_r + v_{r,\rho}}{2}\rho + v_{r,\rho}t_1 + \frac{v_{r,\rho}^2}{2a_{\min,\text{brake}}} - \left(v_f' t_2 + \frac{v_f'^2}{2a_{\max,\text{brake}}}\right). \tag{42}$$

By adding in the distances from the center of mass to the ends of the chassis, compensating for the rotation of each swerving vehicle, an initial gap is sufficient for safety $\forall t$ if

$$g_0 \ge \frac{v_r + v_{r,\rho}}{2}\rho + v_{r,\rho}t_1 + \frac{v_{r,\rho}^2}{2a_{\min,\text{brake}}} - \left(v_f' t_2 + \frac{v_f'^2}{2a_{\max,\text{brake}}}\right) + d' + \bar{d}. \tag{43}$$

Which yields Equation (38).

At $t \ge t_2$, the time at which the lead vehicle begins hard braking, there is enough longitudinal distance to brake for the leading vehicle, as $\hat{g}(t) \ge 0, \forall t \ge t_2$, so the rear vehicle is safe. Since $\hat{g}(t)$ is monotonically decreasing with respect to t, the safe longitudinal distance is satisfied for $t < t_2$, and thus the rear vehicle is safe $\forall t$. ■

E. UNIVERSAL FOLLOWING DISTANCE

The final subproblem addressed in this paper aims to combine the results of the previous sections into a final following distance that can be maintained by all vehicles in a given straight road system to ensure universal safety, assuming the vehicles can brake or swerve as a response to the behavior of other vehicles in front of them. In this sense, this section extends the analysis of the preceding sections into the case of more than two vehicles in a road system. Each vehicle's following distance will be a function of the speed of the vehicle, as well as the speed of the 2 vehicles in front of the vehicle, and the parameters outlined in Section II-A. Denote the distance required to brake for a braking lead vehicle as $d_{b,b}(v_r, v_f, \rho)$, the distance required to swerve for a braking lead vehicle as $d_{b,s}(v_r, v_f, \rho)$, the distance required to swerve for a braking lead vehicle as $d_{s,b}(v_r, v_f, \rho)$, and the distance required to swerve for a swerving lead vehicle as $d_{s,s}(v_r, v_f, \rho)$.

In such a road system, there will be blocks of vehicles where the front vehicle in the block is much farther away from the nearest vehicle in front of it than both $d_{b,b}$ and $d_{s,s}$. Since it is at least this far, it can safely brake or swerve for any vehicle in front of it, and therefore any vehicle in front of it can be ignored. Because of this, these blocks can be considered in isolation, and if each block of vehicles is considered safe, then all vehicles in the road system are considered safe. For any vehicle in a given block, denote its speed by v_1, and the speeds of the first and second vehicles in front of it (if they exist within the block) as v_2 and v_3, respectively. The longitudinal position of each vehicle as a function of time is denoted by $x_1(t)$, $x_2(t)$, and $x_3(t)$. A sufficient safe following distance for each vehicle is then

$$\hat{d}_{\text{long}} = \max\big(d_{s,b}(v_1, v_2, \rho), d_{b,s}(v_1, v_2, \rho), d_{s,s}(v_1, v_3, 2\rho) - d_{s,b}(v_2, v_3, \rho), d_{b,b}(v_1, v_3, 2\rho) - d_{s,b}(v_2, v_3, \rho)\big). \tag{44}$$

Theorem 5: Equation (44) gives a longitudinal safe distance sufficient for universal safety when maintained by all vehicles.

Proof: As mentioned earlier, each block of vehicles can be analyzed individually for safety, and if every block is safe, all vehicles are safe. The safety of any given block can be proved using an inductive argument across all of the vehicles, starting from the front of the block. The following is a proof sketch.

- For the base case, the safety of the first two vehicles is proven when following with at least $\hat{d}_{\text{long}}$.
- For the inductive step, it is assumed the i^{th} agent is following with at least $\hat{d}_{\text{long}}$ and is safe, and it is shown that if the $(i+1)^{\text{th}}$ agent follows with at least $\hat{d}_{\text{long}}$, then it is safe.

1) BASE CASE

The first vehicle at the front of the block is by definition at least $d_{b,b}$ and $d_{s,s}$ from any vehicle in front of it (if such a vehicle exists). As a result, any potential vehicle in front of the first can be safely avoided if necessary with either a brake or a swerve. This means that the first vehicle in the block is safe, and any potential vehicle in front of the first can be safely ignored by all vehicles in the block.

The second vehicle follows the first vehicle at $\hat{d}_{\text{long}}$. If the front vehicle brakes, the second vehicle is at least $d_{s,b}$ away from it, and can swerve to safety. If the front vehicle swerves, the second vehicle is at least $d_{b,s}$ away from it, and can brake safely. The second vehicle will therefore not collide with the first vehicle, and is therefore safe.

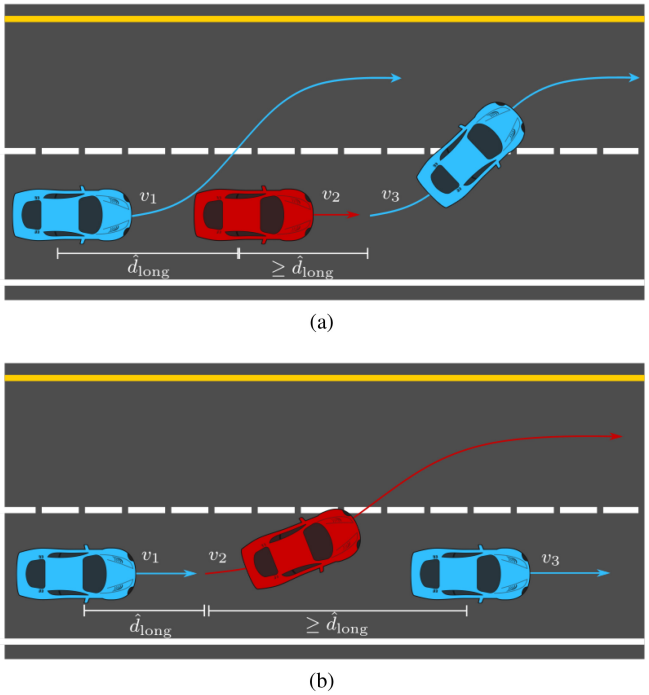

FIGURE 5. (a) Case where the rear vehicle (blue) must swerve for a swerving vehicle 2 cars ahead (blue). The middle vehicle (red) brakes in response to the front vehicle's swerve. The rear vehicle must maintain sufficient distance from both the middle braking and front swerving vehicles. (b) Case where the rear vehicle (blue) must brake for a braking vehicle (blue) 2 cars ahead. The middle vehicle (red) swerves in response to the front vehicle's brake. The rear vehicle must maintain sufficient distance from both the middle swerving and front braking vehicles.

2) INDUCTION

Now, suppose the i^{th} vehicle is following with at least $\hat{d}_{\text{long}}$ of distance, and is safe from the vehicles $(i-1), (i-2), \ldots,$ in front of it. Denote the $(i+1)^{\text{th}}$ as vehicle 1, the i^{th} vehicle as vehicle 2, and the $(i-1)^{\text{th}}$ vehicle as vehicle 3. The distance between vehicle 1 and vehicle 2 is $\hat{d}_{\text{long}}$. If vehicle 2 brakes or swerves, vehicle 1 is at least $d_{s,b}$ and $d_{b,s}$ away from it, and is safe from vehicle 2 if it responds with a swerve or brake, respectively.

If vehicle 1 swerves in response to vehicle 2's brake, there are 2 cases to consider. The first case is if vehicle 3 was braking. Since vehicle 2 was assumed to be safe from vehicle 3, $x_2(t) \leq x_3(t), \forall t$. Combining this with the fact that $d_{s,b}$ is sufficient for vehicle 1 to swerve safely from vehicle 2, vehicle 1 must be safe from vehicle 3 if vehicle 3 brakes.

If vehicle 3 was swerving, $d_{s,s}(v_1, v_3, 2\rho)$ is a sufficient distance for vehicle 1 to follow vehicle 3 to ensure safety. This case is illustrated in Figure 5(a). The reaction delay is doubled to account for the reaction propagating through 2 vehicles instead of the usual one. Since vehicle 2 was assumed to be safe from vehicle 3, $d_{s,b}(v_2, v_3, \rho)$ is a lower bound on vehicle 2's following distance from vehicle 3. This means that in this case, $d_{s,s}(v_1, v_3, 2\rho) - d_{s,b}(v_2, v_3, \rho)$ is a sufficient following distance between vehicle 1 and 2 to guarantee safety.

If vehicle 1 brakes in response to vehicle 2's swerve, as before there are 2 cases to consider. The first case is if vehicle 3 was swerving. As before, since vehicle 2 was assumed to be safe from vehicle 3, $x_2(t) \leq x_3(t), \forall t$. Combining this with the fact that $d_{b,s}$ is sufficient for vehicle 1 to brake safely from vehicle 2's swerve, vehicle 1 must be safe from vehicle 3's swerve.

If vehicle 3 was braking, $d_{b,b}(v_1, v_3, 2\rho)$ is a sufficient distance for vehicle 1 to follow vehicle 3 to ensure safety. This case is illustrated in Figure 5(b). Again, the reaction delay is doubled to account for propagation between two vehicles. Since vehicle 2 was assumed to be safe from vehicle 3, $d_{s,b}(v_2, v_3, \rho)$ is again a lower bound on vehicle 2's following distance. Thus, in this case, $d_{b,b}(v_1, v_3, 2\rho) - d_{s,b}(v_2, v_3, \rho)$ is a sufficient following distance between vehicle 1 and 2 to guarantee safety.

Since $\hat{d}_{\text{long}}$ is greater or equal to each of these following distances, vehicle 1 is safe, and thus the $(i+1)^{\text{th}}$ is safe. By induction, any block of vehicles where each vehicle maintains the following distance given in Equation (44) is safe, and as a result, the entire system is safe. ■

At high speeds, this new following distance can be used to allow for tighter following between agents. At low speeds, the agents can revert to the braking following distance used in the original RSS framework.

If the positions of vehicles 2 and 3, d_2 and d_3 respectively, are known as well as their speeds, the following distance can be improved further. If we denote $d_{2,3} = d_3 - d_2$, then by the same logic in the preceding proof, a sufficient longitudinal

safe distance is

$$\hat{d}_{\text{long}} = \max\big(d_{s,b}(v_1, v_2, \rho), d_{b,s}(v_1, v_2, \rho), d_{s,s}(v_1, v_3, 2\rho) - d_{2,3}, d_{b,b}(v_1, v_3, 2\rho) - d_{2,3}\big). \tag{45}$$

A comparison between the original RSS following distance and these new following distances across a range of speeds is shown in Figure 8. In the plot, all vehicles are moving at the same speed. Since $d_{2,3}$ in Equation (45) can vary, for illustration purposes we assume each vehicle follows the agent in front of it at

$$\hat{d}_{\text{long}} = \max\left(d_{s,b}(v_1, v_2, \rho), d_{b,s}(v_1, v_2, \rho), \frac{d_{s,s}(v_1, v_3, 2\rho)}{2}, \frac{d_{b,b}(v_1, v_3, 2\rho)}{2}\right). \tag{46}$$

This is a particular instance of Equation (45), since $d_{2,3}$ is a free parameter, and is thus safe. This choice of $d_{2,3}$ results in a uniform following distance across all agents when they are moving at the same speed.

V. VALIDATION AND RESULTS

To help us understand the impact of our geometric overapproximations for the kinematic bicycle model, we first compare our computed swerve distances to a lower bound on said swerve distances obtained from a kinematic point mass model. To validate our bicycle model swerve distances, we then use a dynamic vehicle model [8] to see if our computed swerve distances are reasonable approximations. The lower bound is computed and compared to the upper bound distance, as well as the relevant braking distance, in Section V-A. In Section V-B, we compare our swerve clearance distance, as computed in Section IV-B, to swerves from the dynamic model.

A. LOWER BOUND VALIDATION

To compute a lower bound on the longitudinal swerve clearance distance x_c, we use the particle model in Equation (6). We set the minimum a_x and maximum a_y values to be $-a_{\text{min,brake}}$ and $a_{\text{min}}^{\text{lat}}$, respectively, from the bicycle model. This ensures that any acceleration possible under the bicycle model is also possible under the particle model.

For a particle model, maximal lateral acceleration towards y_c as well as maximal longitudinal deceleration leads to lateral clearance in the shortest longitudinal distance $\bar{x}_c$ [16]. Thus, we have that $\bar{x}_c \leq x_c$ for any other maneuver feasible for the particle model.

Finally, for computing the clearance, we use an inner approximation of the vehicle's chassis during rotation. To do so, we use the square inscribed on the circle of radius b_l centered on the center of mass with side length $2d_i'$. This is shown in Figure 3(b). Through this inner approximation, we have that $d_i' \leq d'$ for any possible chassis rotation. This implies that anything the chassis can clear during the swerve will be cleared by the inner square. If we use x_f as in Section IV-B, a lower bound on the longitudinal safe distance, denoted by $\bar{d}_{\text{long}}$, is given by

$$\bar{d}_{\text{long}} = v_r\rho + \frac{1}{2}a_{\text{max,accel}}\rho^2 + \bar{x}_c - x_f. \tag{47}$$

Theorem 6: Equation (47) gives a longitudinal safe distance necessary for safety when swerving for a braking lead vehicle.

Proof: The clearance time and associated longitudinal distance at which point the particle model reaches y_c are given by

$$t_c = \sqrt{\frac{2y_c}{a_{\text{min}}^{\text{lat}}}}, \quad \bar{x}_c = vt_c - \frac{a_{\text{min,brake}}t_c^2}{2} + d_i'. \tag{48}$$

By the acceleration constraints imposed on the particle model, any feasible acceleration in the bicycle model is feasible for the particle model. In addition, the maneuver is optimal with respect to longitudinal distance traveled for the particle model. Both of these points imply that the $\bar{x}_c$ in Equation (48) is a lower bound on any feasible x_c for the bicycle model. Next, the inner approximation implies that for any maneuver, if the chassis can clear, the square with side length $2d_i'$ can clear as well, allowing a buffer of d_i' to be added.

If we denote the initial longitudinal distance between the vehicles as x_2, then the distance between the swerving vehicle and the braking vehicle during the reaction delay is given by $x_2 - d_i' - d_r + v_f t - \frac{1}{2}a_{\text{max,brake}}t^2 - v_r t - \frac{1}{2}a_{\text{max}}t^2$. If we denote the distance between the vehicles at the end of the reaction delay as x_ρ, then after the reaction delay the distance between the vehicles is given by $x_\rho + v_f t - \frac{1}{2}a_{\text{max,brake}}t^2 - v_{r,\rho}t + \frac{1}{2}a_{\text{min,brake}}t^2$. Since $-a_{\text{max,brake}} - a_{\text{max}} < 0$ and $-a_{\text{max,brake}} + a_{\text{min,brake}} < 0$, the distance between the swerving and braking vehicle is concave on both intervals. This implies that the minimum gap occurs at the boundaries of the time intervals $\{0, \rho, t_c\}$. Since the distance between the vehicles is differentiable everywhere, the time ρ is a critical point only if the derivative is zero. In this case, since the distance is concave before and after time ρ, the derivative is positive for $t < \rho$ and negative for $t > \rho$, implying the distance at time ρ is a local maximum. Taking everything together, assuming the vehicles are not already in collision at $t = 0$, this implies that Equation (47) is a lower bound on the longitudinal safe distance required for a swerve feasible for the bicycle model. ■

A comparison between the lower bound and upper bound on the longitudinal distance traveled during a swerve, as well as the equivalent braking distance, is shown in Figure 6. The plot is across a range of initial speeds.

B. DYNAMIC MODEL VALIDATION

Next, we verify that our kinematic approximation is valid by comparing the longitudinal swerve distance under a dynamic model to the distance computed in the preceding sections. We analyze both the cases when the dynamic model is constrained by $a_{\text{min,brake}}$ and $a_{\text{min}}^{\text{lat}}$, and when it is not. We wish to

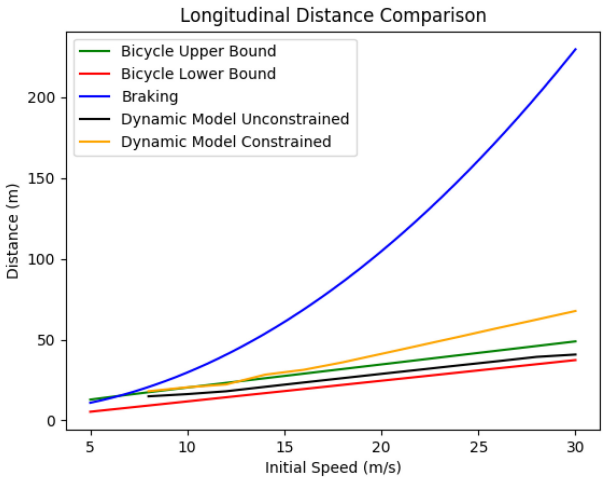

FIGURE 6. A comparison of the longitudinal distance traveled between swerve and brake maneuvers, for varying initial velocities. For very low speeds the dynamic model swerves behave poorly and are omitted.

see how the acceleration constrained bicycle model swerve distances compare to the maneuver distances of a braking and swerving dynamic model. We look at the dynamic model when it has low, comfortable acceleration limits equal to the bicycle model, as well as when it has higher, less constraining acceleration limits that are closer to feasible limits. We would also like to see at which speeds the constrained kinematic bicycle swerve distance is close to the dynamic model swerve distance when the dynamic model is constrained by comfort. We focus on the ability of the dynamic model to swerve, and not an associated controller, and as a result generate the maneuvers in open loop. However, doing a grid search over all possible control inputs to find the best swerves is impractical. Instead, we assume that the steering input is broken into 4 equal length intervals of time, and perform binary search over steering rate magnitudes until the boundary conditions in Equation (12) are satisfied. In addition, we also perform linear search over brake input and the total time of the maneuver and select the maneuver that minimizes the longitudinal swerve distance x_c. Note that these generated swerves are not optimal for the dynamic model, but are feasible.

The parameters used in our validation are summarized in Table 1. We chose $a_{\min,\text{brake}}$ to represent braking at the limit of comfort, and $a_{\max,\text{brake}}$ was chosen to represent a hard, uncomfortable brake. The swerves generated for various initial speeds are illustrated in Figure 7.

Using these computed swerves, we then compute the lateral clearance distance y_c as before and find the longitudinal swerve distance traveled x_c that occurs at time t_c. Substituting this value in at Equations (30) and (36) then gives the required longitudinal safe distance for the dynamic model. For initial vehicle speeds of approximately $5\frac{m}{s}$ or more, swerving is more efficient than braking. For speeds greater than this threshold, the longitudinal safe distances required for the dynamic model are plotted and compared to those computed in Section IV in Figure 6.

TABLE 1. Parameters table.

m	1239 kg	l_f	1.19 m	l_r	1.37 m
I_{zz}	1752 kg · m^2	e_{SP}	0.5 m	R	0.302 m
c_w	0.3	ρ_{drag}	1.25 $\frac{\text{kg}}{\text{m}^3}$	A	1.438
B_f	10.96	C_f	1.3	D_f	4560.4
E_f	-0.5	B_r	12.67	C_r	1.3
D_r	3947.81	E_r	-0.5	$a^{\text{lat}}_{\max}$	4.0 $\frac{\text{m}}{\text{s}^2}$
$a^{\text{lat}}_{\min}$	2.0 $\frac{\text{m}}{\text{s}^2}$	$a_{\min,\text{brake}}$	2.0 $\frac{\text{m}}{\text{s}^2}$	μ	0.1 m
$a_{\max,\text{accel}}$	2.0 $\frac{\text{m}}{\text{s}^2}$	$a_{\max,\text{brake}}$	8.0 $\frac{\text{m}}{\text{s}^2}$	ρ	0.1 s
α	3.7 m	d_r	2.3 m	d_f	2.4 m
b_r	0.9 m	b_l	0.9 m	$\delta_{\max}$	$\frac{\pi}{6}$

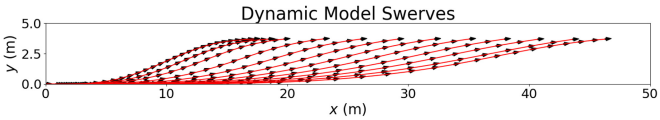

FIGURE 7. The swerve maneuvers generated according to the dynamic model. Each swerve is for a different initial speed in the interval [10, 30] $\frac{\text{m}}{\text{s}}$. The arrows denote the heading of the vehicle.

C. SIMULATION RESULTS

In Figure 6, we compare the braking distance and the swerve longitudinal distance traveled when avoiding a stationary object. This plot illustrates the advantage of swerves; for initial rear vehicle speeds greater than 8 $\frac{\text{m}}{\text{s}}$, the swerves reach safety using less longitudinal distance than braking does. We note that as $a_{\min,\text{brake}}$ is increased, the crossover point of velocity where swerves become advantageous increases as well. However, due to the quadratic nature of the braking distance, swerves always eventually become more advantageous at high speeds. From the figure, we can see that when the accelerations of the dynamic model are constrained, the swerve distance of the kinematic model is a reasonable approximation of the dynamic model, with error between 0.7-7.7%, which is reasonable to expect for a kinematic approximation [23]. In the case where the dynamic model is unconstrained by comfort (only by feasibility), the longitudinal swerve distance required is within 15.6-24.0% error of the upper bound distance of the kinematic model, and is completely bracketed by the kinematic upper and lower bounds across a range of speeds from 8-30 $\frac{\text{m}}{\text{s}}$. This shows that our acceleration constrained kinematic approximation can accurately approximate the swerve distance required by the constrained dynamic single-track model up to mid-ranged initial speeds, and can bound the swerve distance required by the unconstrained dynamic model across the entire range of speeds.

In Figure 8, the universal safe following distance required as clearance when using swerves is compared to the braking following distance, as $a_{\min,\text{brake}}$ is varied from 2, 3, and 4 $\frac{\text{m}}{\text{s}^2}$. In these plots, all vehicles are moving at an equal speed, displayed on the x-axis. These plots show that as the speeds of the vehicles increase, the following distance

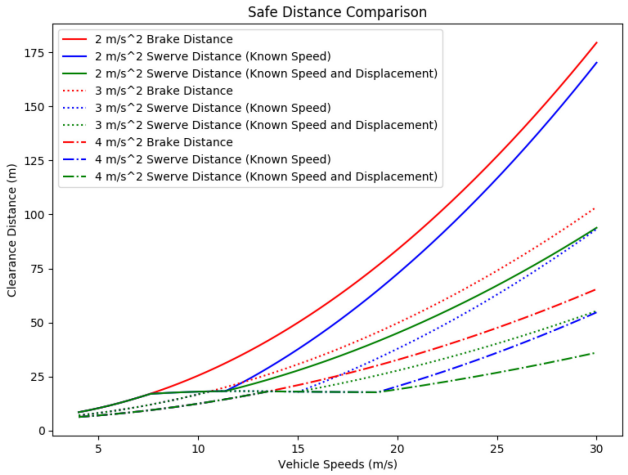

FIGURE 8. The universal following distance required for safety when $a_{\min,\text{brake}}$ is 2, 3, and 4 $\frac{m}{s^2}$. "Brake Distance" is the original RSS following distance, "Swerve Distance (Known Speed)" corresponds to Equation (44), and "Swerve Distance (Known Speed and Displacement)" corresponds to Equation (46).

decreases when allowing swerve maneuvers, when compared to braking alone. As $a_{\min,\text{brake}}$ increases, the speeds where swerves become more effective also increases. For increasing $a_{\min,\text{brake}}$ of 2, 3, and 4 $\frac{\text{m}}{\text{s}^2}$, these speeds are 8.1, 11.4, and 14.6 $\frac{\text{m}}{\text{s}}$, respectively. The universal following distance is also reduced by up to 42% across all 3 values of $a_{\min,\text{brake}}$ when using swerves as opposed to braking alone.

VI. CONCLUSION

In this work, we outlined a method for extending the original RSS framework to include swerve maneuvers in addition to the standard brake maneuver available in the framework. We proved the safety of these maneuvers under a set of reasonable assumptions about responsible behavior, while incorporating the assumptions in the original RSS framework. This extended framework results in an up to 42% reduction in following distance at high speeds (Figure 8). In addition, the kinematic model was shown to conservatively bound the longitudinal distance required for swerves executed for the dynamic model (Figure 6).

In future work, we would like to extend the inclusion of swerve maneuvers to more general cases. One option would be to generalize the swerve maneuver to arbitrary Frenet frames as opposed to straight lines, or to vary road conditions. Extending this work to more complex or articulated vehicle models is also an open problem. One could also compute bounds on the error from using a straight line approximation to the Frenet frame. Further experimental work of the RSS framework and its extensions, through on-car testing or scenario simulation, would also be beneficial.

REFERENCES

[1] E. Thorn, S. Kimmel, and M. Chaka, "A framework for automated driving system testable cases and scenarios," Virgina Tech Transp. Inst., Blacksburg, VA, USA, Rep. DOT HS 812 623, Sep. 2018.

[2] Y. Abeysirigoonawardena, F. Shkurti, and G. Dudek, "Generating adversarial driving scenarios in high-fidelity simulators," in *Proc. Int. Conf. Robot. Autom. (ICRA)*, 2019, pp. 8271–8277.

[3] M. Althoff, D. Althoff, D. Wollherr, and M. Buss, "Safety verification of autonomous vehicles for coordinated evasive maneuvers," in *Proc. IEEE Intell. Veh. Symp.*, 2010, pp. 1078–1083.

[4] M. Althoff and J. M. Dolan, "Online verification of automated road vehicles using reachability analysis," *IEEE Trans. Robot.*, vol. 30, no. 4, pp. 903–918, Aug. 2014.

[5] S. Shalev-Shwartz, S. Shammah, and A. Shashua, "On a formal model of safe and scalable self-driving cars," 2017, *arXiv:1708.06374*.

[6] K. Leung, E. Schmerling, M. Chen, J. Talbot, J. C. Gerdes, and M. Pavone, "On infusing reachability-based safety assurance within probabilistic planning frameworks for human-robot vehicle interactions," in *Proc. Int. Symp. Experimental Robot.*, 2018, pp. 1–12.

[7] R. L. De Iaco, S. L. Smith, and K. Czarnecki, "Safe swerve maneuvers for autonomous driving," in *Proc. IEEE Intell. Veh. Symp.*, 2020, pp. 1941–1948.

[8] M. Gerdts, "Solving mixed-integer optimal control problems by branch & bound: A case study from automobile test-driving with gear shift," *Opt. Control Appl. Methods*, vol. 26, no. 1, pp. 1–18, 2005.

[9] H. B. Pacejka and E. Bakker, "The magic formula tyre model," *Veh. Syst. Dyn.*, vol. 21, pp. 1–18, Aug. 2007

[10] C. Schmidt, F. Oechsle, and W. Branz, "Research on trajectory planning in emergency situations with multiple objects," in *Proc. IEEE Intell. Transp. Syst. Conf.*, 2006, pp. 998–992.

[11] C. Chen, "Optimal path for a car-like robot to reach a given straight line," in *Proc. 21st Int. Conf. Intell. Transp. Syst. (ITSC)*, 2018, pp. 2270–2276.

[12] Z. Shiller and S. Sundar, "Optimal emergency maneuvers of automated vehicles," Inst. Transp. Stud., Univ. California, Berkeley CA, USA, Rep. UCB-ITS-PRR-96-32, Oct. 2005.

[13] Z. Shiller and S. Sundar, "Emergency maneuvers of autonomous vehicles," *IFAC Proc. Vol.*, vol. 29, no. 1, pp. 8089–8094, 1996.

[14] Z. Shiller and S. Sundar, "Emergency maneuvers for AHS vehicles," Warrendale, PA, USA, SAE Int., Tech. Paper, 1995.

[15] P. Dingle and L. Guzzella, "Optimal emergency maneuvers on highways for passenger vehicles with two- and four-wheel active steering," in *Proc. Amer. Control Conf.*, 2010, pp. 5374–5381.

[16] Z. Shiller and S. Sundar, "Emergency lane-change maneuvers of autonomous vehicles," *J. Dyn. Syst. Meas. Control*, vol. 120, no. 1, p. 37, 1998.

[17] H. Jula, E. B. Kosmatopoulos, and P. A. Ioannou, "Collision avoidance analysis for lane changing and merging," *IEEE Trans. Veh. Technol.*, vol. 49, no. 6, pp. 2295–2308, Nov. 2000.

[18] C. Pek, P. Zahn, and M. Althoff, "Verifying the safety of lane change maneuvers of self-driving vehicles based on formalized traffic rules," in *Proc. IEEE Intell. Veh. Symp. (IV)*, 2017, pp. 1–7.

[19] M. Althoff, "Reachability analysis and its application to the safety assessment of autonomous cars," Ph.D. dissertation, Lehrstuhl Steuerungs Regelungstechnik, Technische Universität München, Munich, Germany, 2010.

[20] I. M. Mitchell, A. M. Bayen, and C. J. Tomlin, "A time-dependent hamilton-jacobi formulation of reachable sets for continuous dynamic games," *IEEE Trans. Autom. Control*, vol. 50, no. 7, pp. 947–957, Jul. 2005.

[21] E. Schmerling, K. Leung, W. Vollprecht, and M. Pavone, "Multimodal probabilistic model-based planning for human-robot interaction," in *Proc. IEEE Int. Conf. Robot. Autom. (ICRA)*, 2018, pp. 3399–3406.

[22] J. Kong, M. Pfeiffer, G. Schildbach, and F. Borrelli, "Kinematic and dynamic vehicle models for autonomous driving control design," in *Proc. IEEE Intell. Veh. Symp. (IV)*, 2015, pp. 1094–1099.

[23] P. Polack, F. Altche, B. Dandrea-Novel, and A. D. L. Fortelle, "The kinematic bicycle model: A consistent model for planning feasible trajectories for autonomous vehicles?" in *Proc. IEEE Intell. Veh. Symp.*, 2017, pp. 812–818.

[24] J. M. Snider, "Automatic steering methods for autonomous automobile path tracking," M.S. thesis, Robot. Inst., Carnegie Mellon Univ., Pittsburgh, PA, USA, 2009.

[25] A. D. Luca, G. Oriolo, and C. Samson, "Feedback control of a nonholonomic car-like robot," in *Robot Motion Planning and Control* (Lecture Notes in Control and Information Sciences Robot Motion Planning and Control). Heidelberg, Germany: Springer, 1998, pp. 171–253.